

# Opportunities for resonant elastic X-ray scattering at X-ray free-electron lasers

M. Altarelli<sup>a</sup>

European XFEL GmbH, 22607 Hamburg, Germany

Received 10 November 2011 / Received in final form 23 March 2012  
Published online 15 June 2012

**Abstract.** X-ray Free-Electron Lasers (FELs) are beginning to deliver a revolution in X-ray experiments, thanks to their ultra-bright (peak brightness exceeding  $10^{33}$  photons/s/mm<sup>2</sup>/mrad<sup>2</sup>/0.1% BW), ultrashort (down to a few *fs*), spatially coherent X-ray pulses. Presently operational facilities cover wide spectral ranges, from the VUV and soft X-ray wavelengths of FLASH in Hamburg (down to 4.2 nm), to the hard X-rays delivered by the LCLS in Stanford (wavelengths of 0.15 nm or shorter). The basic properties of the new sources are briefly reviewed, and the impact on resonant scattering experiments is discussed. The perspective of investigating ultrafast magnetism, and, more generally, the time-dependent response of strongly correlated electron systems, in a pump-and-probe mode at the L edges of 3d transition metals, would be very attractive. In the hard X-ray range, the very recent proposal of self-seeded X-ray FELs, with  $10^{-5}$  intrinsic bandwidth, tunable wavelength, 100 fs pulses and number of photons per pulse of order  $10^{12}$  also opens exciting possibilities for resonant scattering.

## 1 Introduction

Synchrotron radiation sources have revolutionized UV and X-ray experiments in many fields of science. The driving force behind the development of light sources is the optimization of their *brilliance* (or spectral brightness), which is the figure of merit for many experiments. In the most modern synchrotron sources (the so-called “third-generation light sources”, such as ESRF, Elettra, Diamond, Swiss Light Source, etc.) the average brilliance of undulator radiation reaches values up to  $10^{19}$ – $10^{20}$  photons/s/mrad<sup>2</sup>/mm<sup>2</sup>/0.1% BW (see for example [1]). Taking into account the pulsed nature of the sources, i.e. the filling patterns and revolution times of storage rings, this corresponds to peak brilliance values of  $\sim 10^{24}$  photons/s/mrad<sup>2</sup>/mm<sup>2</sup>/0.1% BW. In order to achieve such values, two ingredients are essential. The first is the reduction in the phase-space volume of the circulating electrons in the two transverse directions (the horizontal and vertical directions perpendicular to the average orbit). These quantities are called *horizontal (vertical) emittances* and are roughly speaking a measure of the size of the electron bunch times the angular divergences of the corresponding velocity vectors projections in

<sup>a</sup> e-mail: massimo.altarelli@xfel.eu

the horizontal (vertical) plane. Progress in accelerator physics allows reduction of the horizontal emittance to values of order  $\sim 1\mu\text{m} \times \text{mrad}$ . The second ingredient is the extensive use of undulators as radiation sources. In undulators, the radiated power, due to the interference of the different emission points along the trajectory, is concentrated in a spectrum of narrow lines, centered about the wavelengths

$$n\lambda = \frac{\lambda_u}{2\gamma^2}(1 + K^2/2). \quad (1)$$

Here  $n = 1, 2, 3 \dots$  is the order of the harmonic,  $\lambda_u$  is the period of the undulator magnetic structure,  $\gamma$  is the electron energy of the ring, expressed in units of the electron rest energy, and  $K$  is the undulator parameter, a number of order  $\sim 1$  given by  $K = \gamma\theta$ , where  $\theta$  is the maximum angular deviation of the electrons from their unperturbed trajectory induced by the undulator magnetic field. Equation (1) identifies the wavelength of the fundamental harmonic  $\lambda$  as the distance by which one electron lags behind the emitted photons after traveling over the distance  $\lambda_u$  from the emission point.

A substantial reduction of emittance values is hardly possible in storage ring sources, because every photon emission event imparts a random recoil to the electron, and this happens many times at every turn, as each electron goes through all the bending dipoles and undulators around the ring.

Another fundamental limitation of storage rings concerns the length of the bunches, i.e. the duration of the light pulses. Typically, pulse duration in storage rings is limited to some  $\sim 30$  ps, and substantially shorter pulses can only be achieved at the expense of dramatic reductions of the radiated intensity. This poses a limitation to the time scales which can be explored by time-resolved experiments with synchrotron sources: at full power they are limited to the 50 ps time scale; access to the scale of atomic motions and rearrangements (typically, sub-*ps*), is only possible by techniques such as “bunch slicing”, which produce pulses of  $\sim 100$  fs, but with intensities limited to  $\sim 10^3$  photons per pulse, and a few *kHz* pulse repetition rate [2]. On the other hand, there is a high demand for ultrafast experiments capable to explore atomic motions and configuration changes on a sub-*ps* time scale. The development of *fs* lasers in the infrared, the visible and near UV has shown a variety of interesting phenomena essential for the understanding of chemical reactions, phase transitions, etc.; only shorter wavelengths, however, can resolve smaller and smaller distances, and ultimately only X-rays can provide us with atomic position information.

In the following sections we shall discuss X-ray FEL sources, based on *linear* accelerators, which allow generation of transversely coherent ultrashort (typically 10–100 fs) pulses, with a spectacular increase of some nine orders of magnitude in peak brilliance, and review the perspectives that the new sources open for resonant scattering experiments.

## 2 The SASE process and short-wavelength free-electron lasers

In the undulators of a synchrotron source, electrons are forced to follow a zigzag trajectory by the device magnetic field. There is a definite phase relationship between the radiation emitted by *the same* electron at different points of the trajectory, and, since the fields overlap (the angle  $\theta$  of maximum deviation, entering the undulator parameter  $K$  of Eq. (1), is of order  $1/\gamma$ , i.e. of the aperture of the radiation cone) there an interference, which is constructive only for the wavelengths described by Eq. (1). Notice, however, that under such circumstances all interference between the fields radiated by *different* electrons is averaged out, as no definite phase relationship occurs between them. The reason is that electrons are randomly distributed inside the

bunch, with no correlation between positions of *different* electrons. In order to have such interference, electrons should be spatially ordered; considering for simplicity two electrons, if the longitudinal coordinate (projection on the undulator axis of the position) of the second lags behind that of the first by an integer number of wavelengths, the corresponding radiation fields will superpose in phase after the electrons have run through an integer number of undulator periods. The intensity radiated from the two electrons will be *four* times larger than that of one single electron. From these simple considerations one can understand how coherence effects between *different* electrons can arise when the density in the bunch (integrated over the transverse direction) has a substantial Fourier component at the wavelength of the radiation, i.e. when this density shows a modulation at the radiation wavelength. The intensity of the radiation in such cases becomes proportional to the square of the number of electrons involved in the modulation.

For short wavelengths, in the *nm* range or below, controlling the electron density on that scale may appear extremely difficult. However, the radiation does it for us. This *microbunching* phenomenon occurs because the electron velocity has a direction deviating from the undulator axis due to the magnetic field, and therefore the electric field of the radiation (normal to the undulator axis) has a small component parallel (or antiparallel) to the electron velocity, which tends to accelerate some electrons and decelerate those which are positioned one half radiation wavelength ahead or behind, leading to bunching on the radiation wavelength scale. Whenever shot-noise fluctuations in the electron bunch introduce a Fourier component of the appropriate wavelength in the electron density, the coherence effect between electrons described above increases the radiated intensity; it turns out that, for a sufficiently low-emittance and high peak-current electron beam, in a sufficiently long undulator, the stronger radiation field, via the microbunching process, reinforces the density fluctuation, and so on, in a runaway process that leads to exponential amplification of the radiated intensity. The amplification proceeds until *saturation*, which occurs when the intense radiation and subsequent recoil effects lead to a degradation of the electron beam quality that prevents further amplification. This single-pass process, known as Self-Amplified Spontaneous Emission (SASE) was theoretically identified many years ago, long before electron beams of sufficient density and quality were technologically feasible [3–5]. It was shown experimentally in the visible range at the LEUTL facility at Argonne National Laboratory [6], and later pushed to lower and lower wavelengths (down to 4.1 nm) at the FLASH facility at DESY, in Hamburg [7]. Recently, SASE saturation down to 51 nm was also observed at the SCSS test facility at SPring-8 in Japan [8]. One can say however that the 2009 results [9] at the Linac Coherent Light Source (LCLS) at SLAC in Stanford, California, which demonstrated SASE lasing at 0.15 nm, did really open the era of hard X-ray FEL.

The linear accelerator (linac) geometry is essential in allowing the low emittance and the high peak current required for triggering the SASE process. During acceleration in a linac, the normalized emittance  $\epsilon_n = \gamma\epsilon$  is approximately constant, and this implies that the emittance decreases as the energy  $\gamma$  grows. So, if a sufficiently low emittance is available already at the start, i.e. at the electron gun of the injector system, transverse emittances of the order of the radiation wavelength are achievable, at a sufficiently high electron energy. Furthermore, the high peak current can be achieved by compressing the bunch in one or several suitable magnetic chicanes, down to bunch lengths of order 10  $\mu\text{m}$  or durations of 30 fs or less.

### 3 Time-resolved resonant X-ray scattering

Resonant Elastic X-ray Scattering is used to obtain information on structural and magnetic order and also on electronic order parameters such as charge and orbital

order. The availability of FEL sources with ultra-short pulses in the sub-*ps* domain opens up the possibility of exploring these properties in a time-resolved mode on the corresponding time scales. A possible implementation could follow the scheme of pump-and-probe experiments: in this case, a pump pulse, e.g. from an IR or visible laser, triggers a reaction or a phase transformation, or simply drives the system off the equilibrium condition; a probe FEL pulse, following the pump pulse by a prescribed delay, interrogates the system; by repeating the experiment with a sequence of delays, the time evolution of the phenomenon following the trigger pulse is obtained. If a single FEL pulse is not sufficiently intense to acquire the desired information with an acceptable signal-to-noise ratio, the experiment can be performed in a stroboscopic mode: a sequence of pump pulses is applied, each being followed by an FEL pulse after an identical delay (identical, of course, to the extent that the jitter of the two pulses and other experimental constraints allow); the resulting signals are accumulated in order to improve the statistics to a desired level; the procedure is then repeated with a different delay, and so on, until the time dependent evolution of the phenomenon is obtained. Obviously, the interval between successive pump-probe pulse pairs must be long enough to ensure that the system relaxes back to the pre-pump initial equilibrium state.

The stroboscopic procedure is applied for time-dependent studies with ultrafast pulses obtained from synchrotron sources by the “slicing” technique [2,10], as the corresponding 100 fs X-ray pulses contain up to a few thousands of photons only. An example [11] of time-resolved (non-resonant) scattering to probe a structural signature related to electronic degrees of freedom such as the orbital and charge order in LaCaMnO<sub>3</sub> demonstrates the potential to achieve sub-*ps* time resolution with slicing sources. More recently, time-dependent resonant soft X-ray experiments on La<sub>0.5</sub>Sr<sub>1.5</sub>MnO<sub>4</sub> at the *Mn L*-edge, to probe reflections directly related to magnetic and orbital order, were performed [12] using the low- $\alpha$  mode of storage ring operation to shorten bunches to 9 ps, with a corresponding limitation on the time resolution. In either case, the perturbations that the electronic excitations, resulting from absorption of the pump laser pulse, produce on the electronic order parameters is investigated by the probe pulses. The scientific problem that these studies address is therefore the very interesting issue of the connections between different degrees of freedom (structural, electronic, magnetic) in the manganites. It is therefore exciting to consider the impact that FEL sources could have on this class of problems.

The first question to address is whether the high peak brilliance of FELs allows the single-shot acquisition of diffracted intensities. According to the best estimates of performance for the European XFEL soft X-ray SASE3 undulator [13], in the region of the *Mn L*<sub>2,3</sub> edges (around 635 to 665 eV), we can expect, depending on the bunch charge,  $10^{12} - 10^{13}$  photons per pulse, with a pulse duration between 17 fs and 84 fs. The intrinsic bandwidth of the FEL radiation, without any monochromator, is of order 0.4%, i.e. 2.6 eV. This resolution may not be sufficient to explore the detailed fine structure of the resonances, but it should allow to identify the strongest resonant peaks in the diffraction intensity. Estimates of the resonant scattering cross section and the experience of count rates in actual experiments suggest that the single pulse scattered intensity should be observable, corresponding to at least a few thousands of counts. This conclusion is also supported by a pioneering experiment, in which resonant magnetic scattering at the *Co M*<sub>2,3</sub>-edge in a *Co–Pt* multilayer was observed from a single pulse at FLASH [14].

The possibility of single-shot experiments should reduce acquisition times substantially; the ultimate rate at which the pump-probe sequence can be repeated should depend on the time needed by the sample to revert to the original unperturbed situation before the next pump pulse. This time is determined by the experimental configuration (spot size, sample cooling, etc.). Another problem is posed by the

intrinsic pulse-to-pulse intensity and spectral fluctuations of a SASE source; as it was mentioned in Sect. 2, the SASE process is triggered by the amplitude of the density Fourier components of the electron bunch, which randomly fluctuate from bunch to bunch (shot noise). In order to establish the time dependence of a phenomenon by comparing scattered intensities from different pulses, an appropriate monitoring procedure for the intensity and spectral profile of each pulse must be implemented for a proper normalization. This was realized in another groundbreaking experiment on CuO [15] performed at the LCLS, in which the drain current from an Al foil placed in the X-ray beam before the sample was used to normalize the images. In this case, the actual time dependence of a magnetic commensurate-incommensurate transition was followed, by acquiring pump-probe resonant diffraction images at the Cu  $L_3$  edge, from each pulse at 60 Hz.

One further perspective open by the advent of FELs is related to the transverse coherence of the beam. The strongly correlated electron systems discussed above are often characterized by phase separation and mesoscopic inhomogeneities as the system breaks up into the many different phases lying extremely close to one another in the phase diagram. In a scattering process, if the transverse coherence length of the incoming beam at the sample exceeds the characteristic size of domains, speckle features are to be expected in the dependence of the scattering intensity on the wavevector [16, 17]. A plot of the intensity vs. scattering vector displays a very ragged profile, with an overall (linear) extension  $2\pi/\xi$  and individual spikes (*speckles*) of characteristic size  $2\pi/L$  where  $L$  is the linear dimension of the illuminated region of the sample. In principle, the time variations in the domain structure should be reflected in the time variation of the details of the speckle pattern (Photon Correlation Spectroscopy), and here again the short pulse duration may offer tempting capabilities: whereas in the experiment by Turner and *et al.* [17] the coherent photon flux was  $10^{11} \text{ s}^{-1}$ , the same number of coherent photons would be available in an FEL pulse of 20 fs and at the European XFEL such pulses could repeat down to 220 ns separation, giving access to unprecedented time scales in the study of the dynamics. It should be however emphasized that once again sample damage and other experimental problems need to be worked out in detail [18]. One final caveat has to do with the very bad longitudinal coherence properties that in a SASE beam coexist with the exquisite transverse coherence. When the scattering angle is wide, differences in optical path corresponding to parts of the beam scattered by different domains tend to smear out the interference effects that produce speckles, if the longitudinal coherence is low; the very poor monochromaticity and the spiked nature of the SASE pulses [13] must be taken into account.

#### 4 Seeding of the FEL process and pulse-to-pulse reproducibility

In the previous Section we pointed out the features of the pulses generated by a SASE FEL that limit somewhat the possible application of these extraordinary and revolutionary X-ray sources: limited pulse-to-pulse reproducibility, both in intensity and in spectral shape; very poor longitudinal coherence properties and spiked profile of the pulses. All these features arise from the fact that the SASE process is triggered by noise, and therefore subject, by definition, to uncontrolled fluctuations.

The idea of “seeding” the FEL process is to eliminate these problems by starting the coherent emission process not from random fluctuations, but from an external “seed” pulse that imparts a spatial modulation (at the resonant wavelength) much stronger than that induced by shot noise. For VUV and soft X-ray lasers the external modulation uses a conventional lasers, more precisely the harmonics it induces in a non-linear medium (a gas, or the electron bunch itself in a suitable undulator used

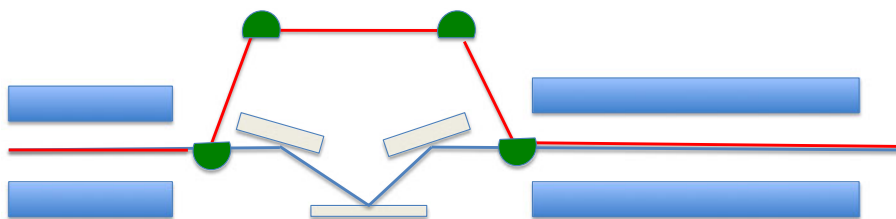


**Fig. 1.** Schematic layout of the arrangement of undulators for self-seeding. The electron and photon beams progress left to right. The electron beam takes the upper path, steered by dipole magnets (depicted as semicircles); the photon beam takes the lower path, through a monochromator.

as modulator). For hard X-ray facilities, however, the harmonic number would have to be very large and the required intensity not accessible. Therefore for hard X-rays, an alternative scheme, “self-seeding” is being pursued [19], in which (see Fig. 1) the undulator is split into an initial section, sufficient to start SASE amplification, but far from saturation (linear regime) and the remainder; between the two sections, a monochromator is inserted, which selects a narrow bandwidth from the first section emission, and an electron beam bypass, to act as an electron delay line. The scheme of self-seeding is preserved in a recent suggestion [20, 21] in which the monochromatization stage is replaced by a single crystal which Bragg diffracts out of the incoming a narrow band; the reflectivity being close to 100% only a small fraction of the original intensity in the Bragg bandwidth reaches the second undulator stage; the dynamical theory of diffraction indicates that the this small transmitted intensity at the Bragg wavelength is trailing the main transmitted pulse by a characteristic delay, of the order of some tens of fs. Geloni *et al.* propose to use this trailing pulse for seeding the electron pulse. Some realistic calculations [21] for the European XFEL show that in the region of 10 keV the number of photons can be as large as  $10^{12}$ – $10^{13}$  per pulse, that is about an order of magnitude more than in the SASE case; what is even more interesting however is that these many photons are in a bandwidth of about 100 meV, that is two orders of magnitude less than in the SASE case. A beam with these features (and with up to 27000 pulses per second) can, without need of further monochromatization, provide an extraordinary source for resonant elastic scattering (and more generally also for non-resonant inelastic scattering). It is to be noted that self-seeding provides this enhancement of intensity and spectacular narrowing of the bandwidth, but pulse-to-pulse intensity fluctuations persist.

The implementation of seeding schemes on the experimental floor, and not only on the simulations by computer requires a lot of work; it will be however a factor of great importance in determining the evolution of the science applications of FELs.

I am grateful to Anders Madsen and to Gianluca Geloni for useful discussions.

## References

1. D.H. Bilderback, P. Elleaume, E. Weckert, *J. Phys. B: At. Mol. Opt. Phys.* **38**, S773 (2005)
2. R.W. Schoenlein, *et al.*, *Science* **287**, 2237 (2000)
3. A.M. Kondratenko, E.L. Saldin, *Sov. Phys. Doklady* **24**, 986 (1979)
4. R. Bonifacio, C. Pellegrini, L.M. Narducci, *Opt. Commun.* **50**, 373 (1984)
5. J.B. Murphy, C. Pellegrini, *Nuclear Instrum. Methods A* **238**, 159 (1985)
6. S.V. Milton, *et al.*, *Science* **292**, 2037 (2001)

7. J. Feldhaus, *J. Phys. B: At. Mol. Opt. Phys.* **43**, 194002 (2010)
8. T. Shintake, et al., *Nature Photonics* **2**, 555 (2008)
9. P. Emma, in Proc. of PAC09, Vancouver, BC, Canada (<http://trshare.triumf.ca/pac09proc/Proceedings/papers/th3pbi01.pdf>)
10. P. Beaud, et al., *Phys. Rev. Lett.* **99**, 174801 (2007)
11. P. Beaud, et al., *Phys. Rev. Lett.* **103**, 155702 (2009)
12. H. Ehrke, et al., *Phys. Rev. Lett.* **106**, 217401 (2011)
13. E.A. Schneidmiller, M.V. Yurkov, DESY Report TESLA-FEL 2011-01 (2011)
14. C. Gutt, et al., *Phys. Rev. B* **81**, 100401 (2010)
15. S.L. Johnson, et al. [[arXiv:1106.6128v3](https://arxiv.org/abs/1106.6128v3)] (2011)
16. C.S. Nelson, et al., *Phys. Rev. B* **66**, 134412 (2002)
17. J.J. Turner, et al., *New J. Phys.* **10**, 053023 (2008)
18. G. Gruebel, et al., *Nucl. Instr. Meth. B* **262**, 357 (2007)
19. J. Feldhaus, et al., *Optics Comm* **140**, 341 (1997)
20. G. Geloni, V. Kocharyan, E. Saldin [[arXiv:1004.4067](https://arxiv.org/abs/1004.4067)]
21. G. Geloni, V. Kocharyan, E. Saldin [[arXiv:1007.2743](https://arxiv.org/abs/1007.2743)]